

## Physical modeling in sand

AMEIR ALTAEE AND BENGT H. FELLENIUS

*Department of Civil Engineering, University of Ottawa, Ottawa, ON K1N 6N5, Canada*

Received January 2, 1993

Accepted February 1, 1994

Small-scale testing under 1g conditions as well as in the centrifuge presupposes that a model and prototype have comparative behavior. The chief condition for agreement between model and prototype is that the initial soil states of both must be at equal proximity to the steady state line. Then, when stresses are normalized to the initial mean stress, the model will in all aspects behave similarly to the prototype. Scaling rules are presented that indicate the relations between stress, strain, and displacement for the model and the prototype in terms of geometric scale and stress scale. An obvious limit of scales is imposed by that the soil in the model can be no looser than the maximum void ratio. Similarly, it must not be denser than a value that corresponds to a prototype soil at the minimum void ratio. Three main areas of application of the approach in engineering practice are identified: design of representative 1g small-scale model tests; reanalysis of data from conventional small-scale tests; and improving the versatility of centrifuge facilities in recognition of the fact that the centrifuge test does not need to be performed at equal levels of stress, when designed according to the new approach.

*Key words:* physical modeling, sand, scaling relations, steady state, centrifuge testing.

Des essais sur modèle réduit sous l'action de la gravité (1g) et sur prototype en centrifugeuse supposent que le modèle réduit et le prototype ont un comportement analogue. La condition principale pour qu'il y ait concordance entre le comportement du modèle et du prototype est que le point représentatif de l'état physique initial du sol doit être à la même distance de la droite d'état critique dans les deux cas. Alors, si les contraintes sont normalisées par rapport à la contrainte initiale moyenne, le modèle et le prototype auront un comportement similaire en tout point. On présente des lois de similitude qui donnent les relations entre les contraintes, les déformations et les déplacements pour le modèle et le prototype en fonction des échelles de géométrie et de contrainte. Une limite évidente des échelles est imposée par le fait que le sol du modèle ne peut être placé à un indice des vides supérieur à l'indice des vides maximum. Par ailleurs, il ne peut être placé à un indice des vides inférieur à celui du prototype placé à l'indice des vides minimum. Trois domaines pratiques d'application de cette approche ont été identifiés : conception d'essais représentatifs de modèles réduits pour des conditions de 1g; ré-analyse de résultats expérimentaux obtenus avec des essais sur modèles réduits conventionnels; et amélioration de la souplesse d'utilisation des centrifugeuses découlant du fait que les essais n'ont pas besoin d'être effectués à des niveaux de contraintes équivalents lorsqu'ils sont conçus en fonction de la nouvelle approche.

*Mots clés :* simulation physique, sable, lois de similitude, état critique, essais en centrifugeuse.

[Traduit par la rédaction]

Can. Geotech. J. 31, 420-431 (1994)

### Introduction

Foundation design can only be advanced by theories that are related to observed foundation behavior. Even designs using well-established theories may require repeated reference to field tests. However, testing a full-scale foundation structure is costly, time-consuming, and often impossible. For these reasons, testing is normally limited to the observation of the behavior of small models that duplicate the actual structure (the prototype) in some proportion.

Physical models are often very small in relation to the prototype structure. For example, a one-foot plate bearing test to determine the soil shear strength that affects the bearing capacity or to find the settlement characteristics of a footing. Or, a test on a group of very small piles to study the distribution of load between piles joined by a common cap.

Under conditions of normal gravity, model tests are easy to perform and cost little. However, when applying the results of a small-scale model test to predict the behavior of a prototype structure, simply scaling the test results to the ratio of geometric size is not sufficient. The prediction must also consider the stress levels acting in the soil of the model test in reference to those at homologous points in the soil of the prototype structure. If this is neglected, the

applicability of the tests results to the intended foundation problem can be substantially reduced.

To overcome the problems associated with 1g model tests, the tests can be made in the centrifuge where centrifugal acceleration replaces the gravity so that the stress at all homologous points of the model is equal to the stress induced by gravity in the actual foundation. The stress gradient of the physical model, that is, the rate of change of stress with depth to that of the prototype is the acceleration in the centrifuge related to a 1g gravity.

As an alternative to centrifuge testing, the gradient of effective stress can be increased by imposing a powerful downward gradient of pore fluid. Such increased stress gradient methods are cheaper than centrifuge tests, but limited to certain types of soils and situations. However, neither the results from a centrifuge test nor the increased stress gradient tests are considered to be directly transferable to a prototype unless the tests are performed with the stress in the model equal to the stress in the prototype at homologous points.

This paper presents a new approach to the design and performance of small-scale model tests in noncohesive soils with due consideration to both the geometric scale and the

stress scale. The approach allows for the extrapolation of results from model tests performed both at normal gravity and in the centrifuge at other than equal stress between model and prototype.

#### Physical modeling in soil

In conventional foundation design, scaling relations have been developed for extrapolation of results obtained from small-scale testing to prototype behavior. For instance, the nonlinear diameter relation of settlement of one-foot test plate to that of a larger footing, or for settlement of a single pile to that of a group of piles. These relations are empirical and, as they combine the effects of geometric scale and stress scale, they do not have general applicability.

Strictly, three different scale ratios apply between a model and a prototype, as follows. The geometric scale ratio  $n$  between the model and the prototype is defined as

$$[1] \quad n = \frac{L_m}{L_p}$$

where  $L_m$  is the length dimension in the model, and  $L_p$  is the length dimension in the prototype. The stress scale ratio  $N$  between the model and the prototype is defined as

$$[2] \quad N = \frac{\sigma'_m}{\sigma'_p}$$

where  $\sigma'_m$  is the effective stress in the model at homologous points, and  $\sigma'_p$  is the effective stress in the prototype at homologous points. The stress-gradient scale ratio  $I$  between the model and the prototype is defined as

$$[3] \quad I = \frac{\dot{\sigma}'_m}{\dot{\sigma}'_p}$$

where  $\dot{\sigma}'_m$  is the effective stress gradient in the model, and  $\dot{\sigma}'_p$  is the effective stress gradient in the prototype. In centrifuge testing,  $I$  is the ratio between the centripetal acceleration and normal gravity  $g$ .

#### Small-scale models under normal gravity conditions

A small model tested under normal gravity conditions is the most common physical tests reported in the literature. Examples of recent small-scale test on bearing capacity of footings have been published by Fragaszy and Lawton (1984), Graham et al. (1984), Haliburton and Lawmaster (1981), and Selvadurai and Rabbaa (1983). Sherif et al. (1984), Milligan (1983), Tumay et al. (1979), and Anderson et al. (1982) reported tests on each pressure against small-scale retaining walls. Hegedus and Khosla (1984), Richter et al. (1984), Elsharnouby and Novak (1984), Chandler and Martins (1982), Yazdanbod et al. (1984), and Chari and Meyerhof (1983) compiled tests on piles and small-scale pile groups.

The majority of the mentioned authors do not make reference to scaling relations and do not suggest how the results can be translated to behavior of the prototype structures. Most perform the model test in a soil that has the same void ratio (density) as the soil of the prototype structure. It appears as if many assume that observed mechanisms are at least qualitatively representative for the prototype. However, as indicated by Scott (1988, 1989), Ko (1988), and others, the extrapolation to full-scale behavior is in most cases unreliable.

#### Centrifuge modeling

A small-scale model made of the same material and hav-

TABLE 1. Scaling relations of centrifuge tests

|                  | Full-scale prototype | Centrifuge model at equal stress level ( $N = 1; I_n = 1$ ) |
|------------------|----------------------|---|
| Linear dimension | 1                    | $n$   |
| Area             | 1                    | $n^2$   |
| Volume           | 1                    | $n^3$   |
| Mass             | 1                    | $n^3$   |
| Acceleration     | 1                    | $1/n$   |
| Stress           | 1                    | 1   |
| Strain           | 1                    | 1   |
| Displacement     | 1                    | $n$   |
| Force            | 1                    | $n^2$   |

NOTE: Everything in the table refers to homologous points of prototype and model (modified after Ko 1988).

ing geometry similar to that of a prototype can be tested in the centrifuge at an acceleration field that simulates the gravity-induced vertical distribution of stress for the prototype. Of course, the test must be performed in a soil identical to that of the prototype in terms of mineralogical composition and gradation. Further, the model must not be so small in relation to the prototype that the grain size (which is not scaled) would have an extraneous effect on the results of the model test.

In centrifuge testing, homologous points in the geometrically identical small-scale model and full-scale prototype are subjected to the same stresses. Hence, the model develops the same strains as those in the prototype. Notice, the practice is to perform the tests with soil of the same initial density as the prototype soil.

The results of the centrifuge test are extrapolated to predict the behavior of the prototype using the scaling relations presented in Table 1.

In conventional centrifuge testing, the product of the stress-gradient scale and the geometric scale are equal to unity. The stresses and strains at homologous points in the prototype and model are then identical and the displacement ratio between the model and the prototype will be equal to  $n$ . The tests are performed at a void ratio equal to that of the prototype condition.

Problems associated with centrifuge testing have been discussed by Cheney (1985), Tan and Scott (1985), Scott (1989), Whitman and Arulandan (1985), and Ko (1988).

#### Increased stress-gradient method

The increased stress-gradient method (Zelikson 1969; Yan and Byrne 1989, 1991) scales the vertical stress distribution by imposing a downward flow with a large, positive pressure gradient in the pore fluid in saturated soils used in the model. For a soil that is subjected to a vertical pore fluid pressure gradient  $i$ , the effective stress in the soil will be

$$[4] \quad \sigma' = \sigma - \gamma_w h(1 - i)$$

where  $\sigma'$  is the effective stress in the model;  $\sigma$  is the total stress in the model;  $\gamma_w h$  is the hydrostatic head of the fluid in the model; and  $i$  is the pore fluid pressure gradient in the model, defined positive in downward flow and negative in upward flow.

For proper modeling of the prototype conditions, the product of the geometric scale ratio  $n$  and the stress-gradient

ratio  $I$  must be equal to unity. Then, the displacement ratio between the model and the prototype will be equal to the geometric scale ratio  $n$ .

Zelikson (1978, 1988) applied the increased-gradient method to tests on anchors and piles, Yan and Byrne (1989, 1991) applied it to model footings, and Zelikson and Leguay (1986) compared the method with centrifuge tests.

#### Selection of reference state for scaling

Because of the nonlinear stress-strain behavior and the dependence of behavior on initial level of confining stress, small-scale physical modeling under 1g conditions has little relevance to the behavior of a full-scale prototype. Moreover, for a specific prototype, small-scale modeling in the centrifuge or by means of the increased stress-gradient test is only directly relevant when the geometric scale ratio  $n$  is inverse to the stress-gradient  $I$ . This requirement may be difficult or costly to meet, however. Therefore, there is a need for a set of scaling rules that would allow the results from low-cost, easy to perform, small-scale model tests representative of the behavior of a full-scale foundation without having to maintain the inverse proportionality between  $n$  and  $I$ .

In brief, use of small-scale models requires a scaling relation between stress and strain that builds on an understanding of how the void ratio (density) of the soil changes following a change of stress. The fundamental understanding of the effect on change of soil volume due to a change of shear stress was introduced by Casagrande (1936). Casagrande coined the term "critical void ratio" or "critical density," which is the void ratio or density of a soil subjected to continuous shear under neither dilatant nor contractant behavior. The original state of a soil is either contractant (typical of a loose soil), which means that when sheared it will reduce in volume, i.e., its original density is smaller than the critical, or it is dilatant (typical of a dense soil), which means that when sheared it will increase in volume, i.e., original density is larger than the critical. Thus, the volume change of a soil element subjected to shear is controlled not by the initial void ratio (a constant) alone, but by the void ratio in relation to the critical void ratio. The latter is a variable that changes with the change in the level of mean stress. An important consequence is that neither is the density index ("relative index") a precise parameter, as will be addressed in the following.

Lee and Seed (1967) showed that a soil of a certain density that is dilatant at low mean stress could be contractant at a larger mean stress and that dense sand, if tested at sufficiently high mean stress, will behave similarly to a loose sand.

#### Critical state

Roscoe et al. (1958) developed the Casagrande concept of critical void ratio and critical density into defining a state at which the soil continues to deform at constant stress and constant void ratio, calling this state the "critical state." The new concept was based on the results of extensive laboratory testing of remolded clays. The approach was later found valid also for noncohesive soils. Studies were published by Wroth and Basset (1965), Cole (1967), Schofield and Wroth (1968), and Stroud (1971). Bishop and Henkel (1962) presented results from tests performed on very loose and dense sands which very clearly demonstrate the critical state (although the authors did not specifically use the

term). More recently, Been et al. (1991) published results of a study on steady state in sand.

According to Schofield and Wroth (1968), the critical state has a location in the  $p$ - $q$ - $e$  space given by the following:

$$[5] \quad q = M_c p \quad \text{if} \quad q > 0$$

$$[6] \quad q = M_e p \quad \text{if} \quad q < 0$$

$$[7] \quad e = \Gamma + \lambda \ln \left( \frac{p}{p_r} \right)$$

where  $q$  is the deviator stress ( $\sigma_1 - \sigma_3$ );  $p$  is the mean effective stress ( $\sigma_1 + \sigma_2 + \sigma_3$ )/3;  $e$  is the void ratio;  $\sigma_1$ ,  $\sigma_2$ , and  $\sigma_3$  are the major, intermediate, and minor principal effective stresses;  $\Gamma$  is the void ratio at the reference mean stress (100 kPa);  $\lambda$  is the slope of the critical state line in an  $e$ - $\ln(p)$  plane;  $M_c$  is the slope of critical state line in the  $q$ - $p$  plane, positive deviator stress;  $M_e$  is the slope of critical state line in the  $q$ - $p$  plane, negative deviator stress; and  $p_r$  is the reference mean stress (100 kPa).

The slopes  $M_c$  and  $M_e$  are related to the effective angle of friction of the soil. The reference mean stress  $p_r$  is set equal to 100 kPa to enable earlier steady state lines referenced to 1 kg/cm<sup>2</sup> (1 atm) to be directly comparable.

Roscoe and Poorooshasb (1963) applied critical state principles to tests on remolded clays and artificial soils made up of steel balls and indicated by means of a formula that the void ratio proximity (denoted  $e'$ ) to the critical state line at the initial mean stresses must be the same for the model and the prototype. Roscoe and Poorooshasb (1963) also wrote that "it is believed this theory can be extended to apply to cohesionless soils." It is surprising that no one appears to have prepared a further development of their approach during the 30 years since the paper was published.

Scott (1989) discussed testing in the centrifuge and examined concepts and scaling relations for 1g and higher relations with respect to the applicability to assess prototype behavior. Scott used the approach by Roscoe and Poorooshasb (1963), but exchanged the void ratio difference for the density index (relative density). However, as shown by Been and Jefferies (1985) and by Ishihara et al. (1991), the density index is not a constructive parameter to use.

The research into critical state has centred on tests on clays rather than on sands. The reason could lie in experimental difficulties associated with establishing the critical state for sands. As observed by Lade (1982), strains within a sand sample may become nonuniform due to the formation of shear bands. The conventional volume-change measurement during drained testing of a saturated sample underestimates the volumetric strain in the shear band. Therefore, the quality of the testing apparatus becomes very important and conventional equipment does not normally possess sufficient accuracy for reliable determination of the critical state of a sand. J. Chu (personal communication, 1993) presented a method for determining the critical state line in triaxial testing that enables the state of dense sand to be measured in the homogenous-deformation region. However, experimental works that support the presence of critical state in sands have been published (e.g., Wroth and Basset 1965; Cole 1967; Stroud 1971; Been et al. 1991).

#### Steady state

Poulos (1981) defined a concept of steady state deformation of soil as "the state in which the mass is continu-

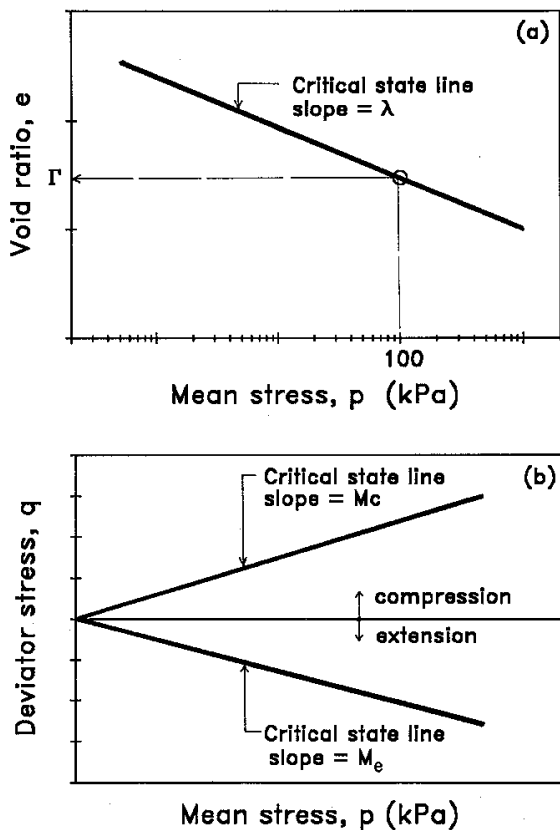


FIG. 1. Location of critical state line in (a) void ratio vs. mean stress plane, and (b) deviator stress vs. mean stress plane.

ously deforming at constant volume, constant normal effective stress, constant shear stress, and constant velocity." This definition is a further development of the definition used by Roscoe et al. (1958) for the critical state concept, i.e., curbing, or restraining, the original.

The steady state line is defined as the locus of all points in the void ratio – mean stress plane, which is a line for where a soil mass deforms under conditions of constant effective stress, void ratio, and velocity. Each single point on the plane can be determined by conducting a consolidated undrained triaxial test on a soil sample. Usually, the steady state condition for sand occurs after liquefaction of the sample is induced in the triaxial test.

For example, Fig. 2 shows the deviator stress and pore-water pressure measured during a consolidated undrained triaxial test on Kogyuk 350 sand from the Beaufort Sea (Been and Jefferies 1985). In this test, the steady state was reached at an axial strain of about 15%. The initial state of the sample (after consolidation and prior to shearing) is represented by an initial void ratio of 0.763 and an initial effective mean stress of 330 kPa. The results shown in Fig. 2 are from a series of triaxial tests determining the steady state line. The initial state of the sample is indicated by a point well above the steady state line. In the test, the sample developed a strong tendency to contract (and liquefy) manifested by large pore-water pressure and reduction of

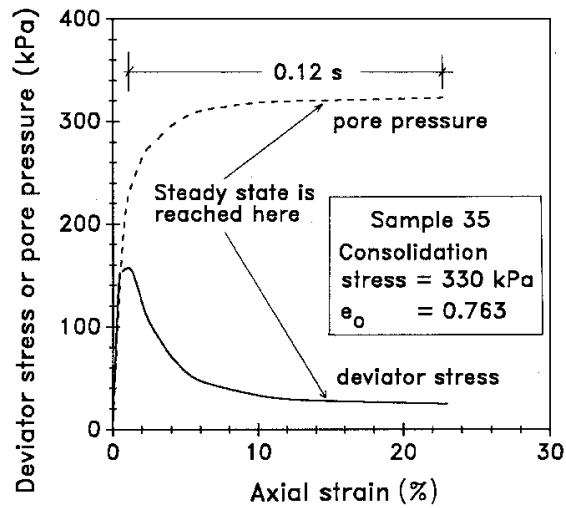


FIG. 2. Consolidated undrained triaxial response of sample 35 of Kogyuk 350/2 sand with an initial state above the steady state line (modified after Been and Jefferies 1985).

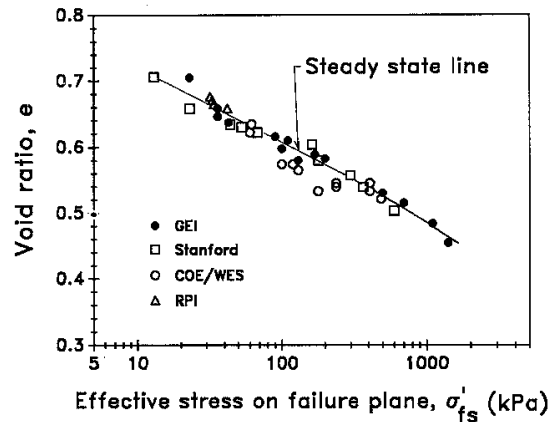


FIG. 3. Steady state of hydraulic fill from the lower San Fernando Dam determined from tests performed by four independent laboratories (data from Castro et al. 1992).

the effective stress, causing the mean effective stress to reduce and bringing the sample to its steady state.

The steady state is defined in an  $e - \ln(p)$  plot similar to that showing the critical state (Fig. 1). The same symbols  $\lambda$  and  $\Gamma$  are used for the parameters defining the line. The slope  $\lambda$  of the line is affected by grain shape, while the position  $\Gamma$  of the line is influenced by the grain-size distribution (Castro et al. 1992).

Some researchers have claimed that a unique steady state line would not exist for a sand; the steady state would vary with stress path, drainage condition during testing, testing method (e.g., stress-controlled versus strain-controlled), and method of sample preparation, among other factors (Alarcon-Guzman et al. 1988; Alarcon-Guzman and Leonards 1988; Dennis 1988; Pilecki 1988; Pyke 1988; Vaid et al. 1990). However, others have demonstrated that a unique steady state line does exist for a given sand when the factors listed

TABLE 2. Basic steady state parameters for different cohesionless soils

| Soil                                       | Slope of steady state line in $e - \ln(p)$ | Void ratio at 100 kPa stress | Reference                                |
|--|--|------------------------------|--|
| Sacramento River sand                      | -0.077                                     | 0.965                        | Lee and Seed 1967                        |
| Fuji River sand                            | -0.120                                     | 0.919                        | Tatsuoka and Ishihara 1975               |
| Crushed quartz 430/0 <sup>a</sup>          | -0.036                                     | 0.925                        | Altaee 1991                              |
| Sandy silt                                 | -0.120                                     | 0.790                        | Desai and Siriwardane 1984               |
| Leighton Buzzard sand                      | -0.025                                     | 0.927                        | Budhu and Britto 1987                    |
| Kogyuk 350/0 <sup>a</sup>                  | -0.007                                     | 0.754                        | Been and Jefferies 1985                  |
| Kogyuk 350/2 <sup>a</sup>                  | -0.029                                     | 0.713                        | Been and Jefferies 1985                  |
| Kogyuk 350/5 <sup>a</sup>                  | -0.045                                     | 0.716                        | Been and Jefferies 1985                  |
| Kogyuk 350/10 <sup>a</sup>                 | -0.090                                     | 0.682                        | Been and Jefferies 1985                  |
| Erksak 330/0.7 <sup>a</sup>                | -0.012                                     | 0.756                        | Been et al. 1991                         |
| Toyoura sand                               | -0.038                                     | 0.873                        | Been et al. 1991                         |
| Hydraulic fill from lower San Fernando Dam | -0.063                                     | 0.630                        | Castro et al. 1992                       |
| Mol sand                                   | -0.050                                     | 0.840                        | W. VanImpe, personal communication, 1993 |
| Antwerpian sand                            | -0.148                                     | 0.920                        | W. VanImpe, personal communication, 1993 |
| Toyoura sand                               | -0.095                                     | 0.905                        | Ishihara et al. 1991                     |
| Sydney sand                                | -0.042                                     | 0.830                        | J. Chu, personal communication, 1993     |

<sup>a</sup>The numbers indicate  $d_{50}$  sand diameter ( $\mu\text{m}$ ) and fines content (%), respectively.

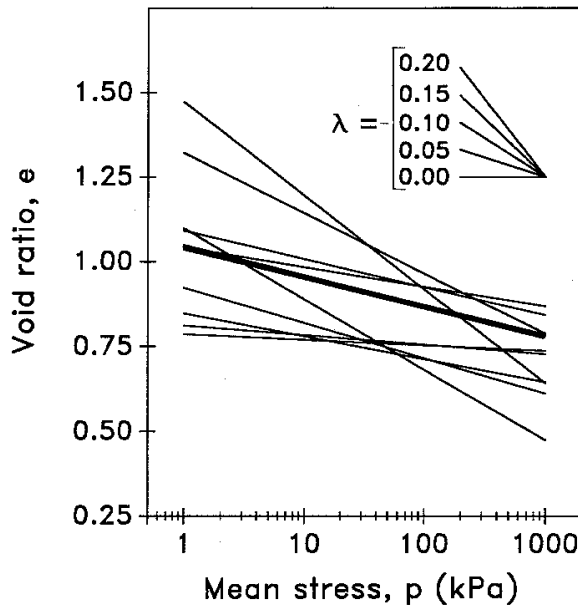


FIG. 4. Steady state lines of different noncohesive soils as listed in Table 2.

by the first group of researchers are taken into consideration, as follows.

Poulos et al. (1988) investigated the behavior of very uniform, fine, angular, quartz sand composed of tailings from tar-sand operations. Strain-controlled as well as load-controlled and drained as well as undrained tests were performed under isotropic and anisotropic consolidated conditions. The tests demonstrated the existence of a unique steady state line for this soil.

Ishihara et al. (1991) established the steady state line of Toyoura sand (Japanese standard sand) from consolidated,

undrained triaxial tests, obtaining at least three to four points on the line, with each point determined from the average of a minimum of four tests on a sample of equal initial void ratio and different initial effective mean stress.

Been et al. (1991) demonstrated the existence of a unique steady state line for Erksak sand, a uniformly graded, medium to fine quartz sand dredged from the Erksak borrow area in the Beaufort Sea. Different techniques were used to prepare the test samples, and the results of the study suggested that the steady state and the critical state are equal and independent of stress path, sample preparation, testing method, and initial density.

Castro et al. (1992) investigated hydraulic fill from the lower San Fernando Dam and had testing performed by four independent laboratories. A compilation of the results is shown in Fig. 3, suggesting a unique steady state line. A variety of testing procedures were employed to determine the steady state line for this soil: drained and undrained tests on isotropic and anisotropic consolidated samples, compacted moist samples, pluviated samples, and samples consolidated from slurry.

McRoberts and Sladen (1992) discussed some of the practical aspects of using the steady state concept in sand for liquefaction studies, suggesting that emphasis should be placed on determining pertinent in situ soil parameters and on the sensitivity of the calculations of soil behavior on these parameters rather than on the agreement between model analysis and prototype behavior.

Figure 4 shows a compilation of steady state lines in  $e - \ln(p)$  plane obtained by several researchers testing different noncohesive soils. The data used to generate the lines are given in Table 2. The diagram demonstrates that there exists a great deal of variation in the location and slope of steady state lines determined for different soils. The thick marked steady state line in this figure belongs to a crushed quartz sand used for experimental research projects at the University of Ottawa. This soil has a steady state line in the  $e - \ln(p)$  plane with slope equal to  $-0.036$  and a void ratio of 100 kPa mean stress of 0.925.

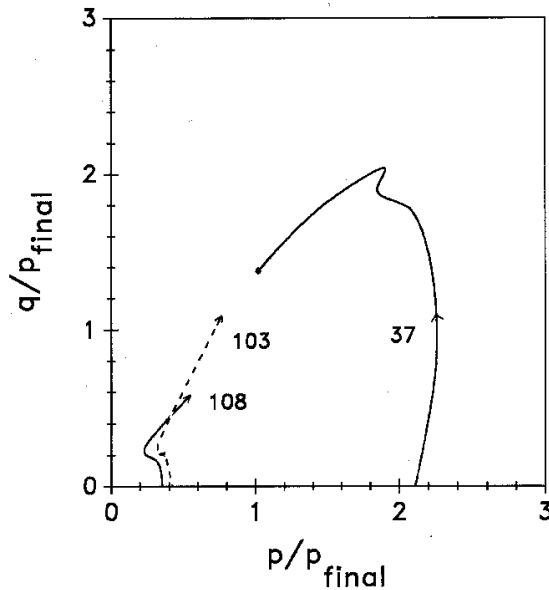


FIG. 5. Normalized deviator stress vs. normalized mean stress of three samples of Kogyuk 350/2 sand (tests 37, 103, and 108) during consolidated undrained triaxial tests (modified after Been and Jefferies 1985).

Been and Jefferies (1985) reported results from conventional undrained triaxial tests on sands from the Beaufort Sea (Kogyuk 350 sand) and varied parameters, such as fines contents, initial void ratio, drainage condition, and initial mean stress. The results showed that tests performed on soils with identical grain-size distribution at different values of initial mean stress, but with the same initial void ratio (i.e., equal density index—"relative density"), gave very different results in terms of stress-strain behavior and strength. In contrast, tests performed at different values of initial mean stress and void ratio, but with the samples tested at an initial void ratio that had the same void ratio difference to the steady state line, showed similar behavior from test to test.

Been and Jefferies (1985) showed that the peak angle of shearing resistance of the Kogyuk sand could be correlated to the void-ratio difference above or below the steady state line. At values below the line (dilatant behavior of the sand in shear), the angle was high. The peak-angle values reduced when the initial void ratio was increased, so the initial state was represented by a point above the steady state line, the zone of contractant behavior. No such correlation could be established from other common engineering parameters used to express the initial condition of the sand, such as loose, dense, etc., and density index (relative density).

The latter is demonstrated in Fig. 5, showing that when Been and Jefferies (1985) normalized the deviator stress and the mean stress to the mean stress at the steady state (final mean stress), the stress paths in the  $q$ - $p$  plane of tests 103 and 108 become similar. For these two tests, the soil had been prepared to a void ratio that had the same initial distance to the steady state line, but the initial void ratios were very different (see Table 3). The behavior contrasts with that of test 37, which had the same initial void ratio as

TABLE 3. Values of parameters for three samples of Kogyuk sand during consolidated undrained triaxial tests

| Test No. | Void ratio | $p_{\text{initial}}$ (kPa) | Density index (%) | Void ratio difference |
|----------|------------|----------------------------|-------------------|-----------------------|
| 37       | 0.71       | 350                        | 33                | +0.030                |
| 103      | 0.71       | 50                         | 33                | -0.030                |
| 108      | 0.65       | 300                        | 50                | -0.033                |

test 103 but a different distance to the steady state line. The initial state of test 37 plots above the line and the sample will, therefore, contract when sheared, whereas the initial state of test 103 plots below the line and the sample will dilate. In agreement with a suggestion of Castro and Poulos (1977), Been and Jefferies (1985) concluded that the density index of the sand is not a useful parameter for evaluating soil behavior. They suggested that, instead, the void-ratio difference may be "a first order steady state parameter with widespread applicability on the engineering design of sand structures" and that sands "tested under different combinations of void ratio and mean effective stress, behave similarly if test conditions assure an equal proximity to the steady state."

Ishihara et al. (1991) recognized the importance of the void ratio difference when extrapolating results from shaking-table testing to full-scale situations and criticized the use of the density index as a parameter for this purpose.

When conducting drained tests in the laboratory, the final mean stress is difficult to reach. Therefore, it is more useful to normalize to the initial mean stress as opposed to the final mean stress. The effective stress path shown in Fig. 5 would have given essentially the same result if normalized to the initial mean stress.

When considering the stress-strain behavior (not discussed by Been and Jefferies 1985), the normalizing of the stress to the initial mean stress is a very useful approach to demonstrate the importance of the relation between the initial void ratio to the steady state line, not just for the liquefaction potential, but generally in physical and theoretical modeling. As to the behavior of the prototype, the initial mean stress is always known, but the stresses during loading and the final mean stress are not. Therefore, the initial mean stress is the more important and useful parameter.

#### New approach to physical modeling

In a broad sense, the concepts behind the three mentioned reference states, namely the critical void ratio, the critical state, and the steady state, are so similar that they can be said to be one and the same and to differ only by the method and definition for how to determine the state experimentally. In the following, "steady state" will be the term used for the reference state.

The steady state satisfies the conditions for use as a reference state for physical modeling: the state is unique for a soil and it is relatively easily established experimentally. The following example illustrates how the behavior of a noncohesive soil is a function of its initial location in the  $e - \ln(p)$  plane and its vertical distance (void ratio difference) to the steady state line, which difference the authors call the "upsilon difference" or the "upsilon parameter," positive above and negative below the steady state line. This is

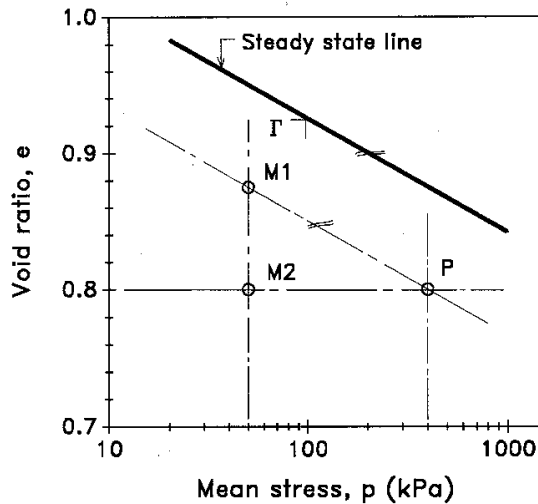


FIG. 6. Initial (preshearing) void ratio and mean stress of samples P, M1, and M2 with respect to the steady state line of the crushed quartz 430/0 sand.

the same parameter that Roscoe and Poorooshasb (1963) called “ $e$ -prime” and Been and Jefferies (1985) called “the state parameter.” It is acknowledged that the foundations of the new approach were laid by Roscoe and Poorooshasb (1963).

The importance of the epsilon parameter is demonstrated by the results of three conventional drained triaxial compression tests on a crushed quartz sand subjected to tests of identical stress paths. The samples, samples P, M1, and M2, were tested at different initial void ratios and initial mean stresses. The sample height and diameter were 100 and 50 mm, respectively, and the tests were performed by means of a computer-controlled system.

The steady state line of the sand had been established by means of several tests (Altaee 1991) to a slope of  $-0.036$  and a void ratio of  $0.925$  at a mean stress of  $100$  kPa. Figure 6 shows the steady state  $e - \ln(p)$  diagram of the sand and the initial states of the samples as three points (P, M1, and M2). The line can be compared with the other steady state lines for noncohesive soils in Fig. 4 where it is the line drawn thicker than the others.

Sample P is meant to represent a prototype situation and samples M1 and M2 represent model-scale tests of the prototype situation. Sample M1 was prepared to the same initial value of the epsilon parameter as that of the prototype, sample P, whereas sample M2 was prepared to the same initial void ratio as that of the prototype, sample P. The samples M1 and M2 were consolidated to the same initial mean stress, a stress much smaller than that for sample P.

Figure 7 presents the peak-strength Mohr circles from the three triaxial tests. Note that the same-density tests, M2 and P, could indicate a “curved” envelope reducing from a friction angle  $\phi$  of  $42^\circ$  at low stress through  $39^\circ$  at high stress. In contrast, test M1 (same epsilon value as the prototype) has the same peak-strength friction angle as the prototype, that is, the envelope is straight, not curved. However, the aspect of testing at the same epsilon parameter does not just address the peak strength, but the entire behavior of

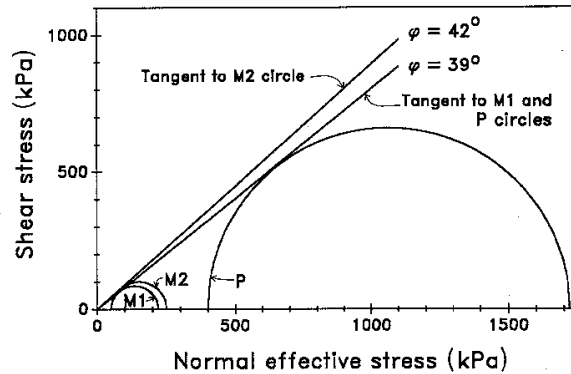


FIG. 7. Mohr circles of samples P, M1, and M2 (crushed quartz 430/0 sand) at peak strength.

the soil. This observation is of utmost importance for the principles of physical modeling.

Figure 8 shows the responses of the three samples, as follows. Figure 8a shows the deviator stress  $q$  versus axial strain responses ( $q = \sigma_1 - \sigma_3$ ). Sample P exhibits higher deviator stress than samples M1 and M2 because of the higher initial confining stress (initial mean stress) for the prototype as opposed to the stress for the models (both models have the same initial confining stress and, therefore, approximately similar deviator stress versus strain curves). All three tests showed a reduction in the deviator stress, that is, strain softening, beyond about 11% axial strain.

Judging from Fig. 8a, it appears as if the stress-strain behavior of the prototype would be very different to that of the two models. Further, the models behaved similarly, which could imply that their different initial void ratios would be unimportant. However, when the deviator stress is normalized with respect to the corresponding initial mean stress ( $p_{\text{initial}}$ ), the correct picture emerges. As shown in Fig. 8b, the curves representing samples P and M1 have the same epsilon parameter and, therefore, their normalized behaviors are practically identical. Sample M2, on the other hand, exhibits a higher normalized stress-strain curve because of its larger initial epsilon parameter. It is evident that normalizing with respect to the initial mean stress provides results that substantially improve the understanding of soil behavior and, furthermore, it clearly indicates the importance of the epsilon parameter in physical modeling.

A similar observation can be made with respect to the volumetric strain versus axial strain response as presented in Fig. 8c. Because samples P and M1 have the same epsilon parameter, their contraction and dilation behavior is identical also (no normalization with respect to initial confining stress is required in this case because there is no stress involved in the relations of Fig. 8c).

The initial mean stress of the prototype (sample P) is  $400$  kPa and the initial mean stress of the models (samples M1 and M2) is  $50$  kPa. Therefore, the model to prototype stress scale ratio  $N$  is  $1/8$  for both samples M1 and M2.

Sample M2 has the same density as the prototype and represents the current *conventional* 1g small-scale model. As illustrated in Figs. 9a–9c, the behavior of the sample M2 model differs significantly from that of the prototype (sample P) with regard to both deviator stress versus axial strain

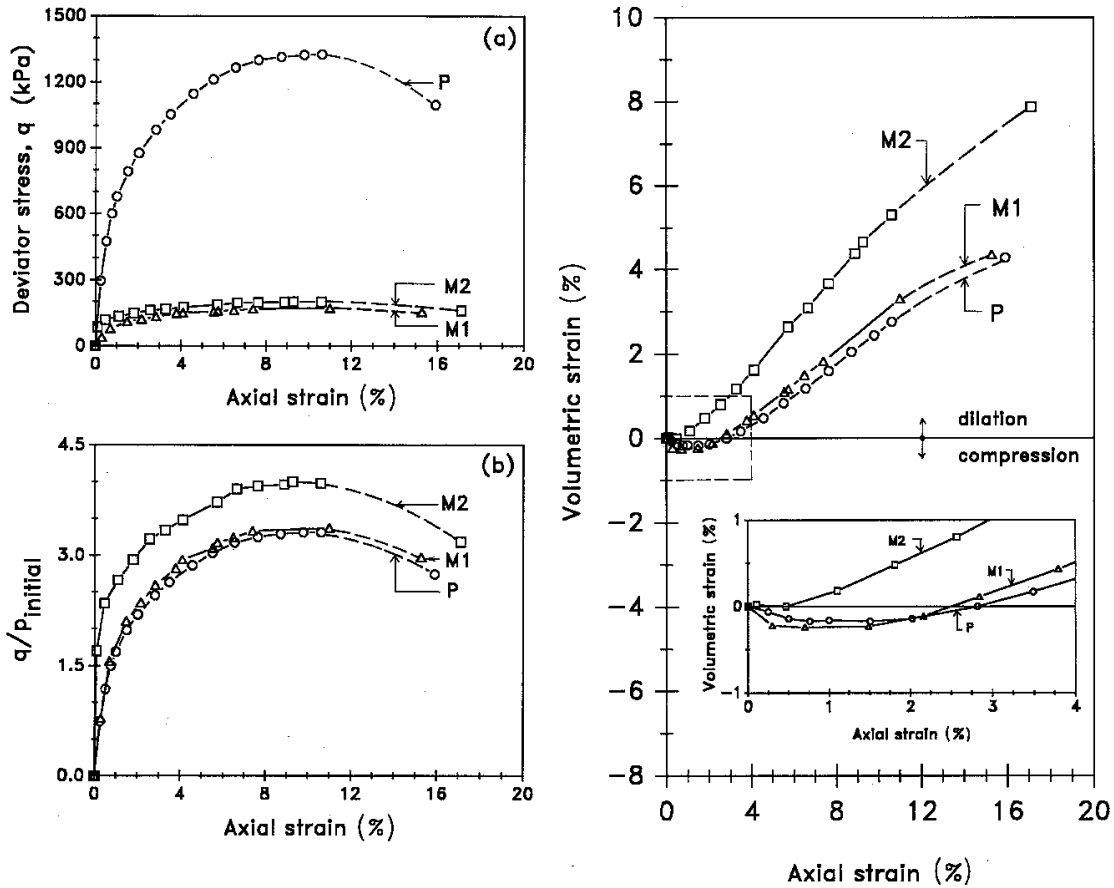


FIG. 8. Triaxial drained response of samples P, M1, and M2 (crushed quartz 430/0 sand). (a) Deviator stress vs. axial strain. (b) Normalized deviator stress vs. axial strain. (c) Volumetric strain vs. axial strain.

and volumetric strain versus axial strain. It follows, therefore, that soil parameters determined from a soil of the sample M2 state will not correctly serve to describe the behavior of a prototype in a soil of the sample P state.

In contrast, the normalized behavior of the sample M1 model is identical to that of the prototype. The authors put forth that, in fact, sample M1 is a true 1g small-scale model performed at a stress scale and at the state that correctly simulates the behavior of the prototype soil (assuming, of course, that also the geometric scale satisfies the scaling rules). That is, the principles for physical modeling for scaling stress and strain of geometrically smaller models build on integrating the upsilon parameter in the scaling of geometry and stress, as detailed in the following.

To model a prototype soil of a given initial state defined by void ratio, mean effective stress, and relation to the steady state line, there exists an infinite number of initial model states. Each such state, when tested following the same stress and (or) strain path, shows the same behavior if the data are normalized with respect to the initial mean effective stress of each state. Therefore, a line drawn parallel to the steady state line of the soil and through the initial state defines the locus of the infinite number of initial states that correspond to the initial state. In fact, the upsilon param-

eter is the common characteristic of all states located along the line parallel to the steady state line.

Similar to the centrifuge testing and the increased stress gradient methods, scaling relations are required to transform test data from model to that of prototype. Scaling relations that combine the geometric scale and the stress scale are proposed in Table 4. The geometric scale  $n$  represents the ratio of the linear dimension in the small-scale model to the corresponding length in the full-scale prototype. The stress scale  $N$  is the ratio of the mean stress at a certain depth in the model to the mean stress of the homologous depth in the prototype.

The overburden stress at a given depth  $nD$  below a small-scale model at a geometric scale  $n$  is smaller than  $N$  times the stress at a depth  $D$  below the prototype. This is so because for the model, stress is reached by summation from  $z = 0$  through  $z = nD$ , whereas for the prototype, the summation is from  $z = 0$  through  $z = D$ . The stress in the model at this depth is  $nD\gamma_m$ . In the prototype, it is  $\gamma_p D$ . Therefore, assuming that the mean stress is proportional to the overburden stress for both model and prototype, for a given ratio of geometric scale  $n$ , the stress scale ratio  $N$  is equal to the ratio  $\gamma_p/\gamma_m$ . As the two unit weights are not equal (depending on the particular distances to the steady state line and cor-



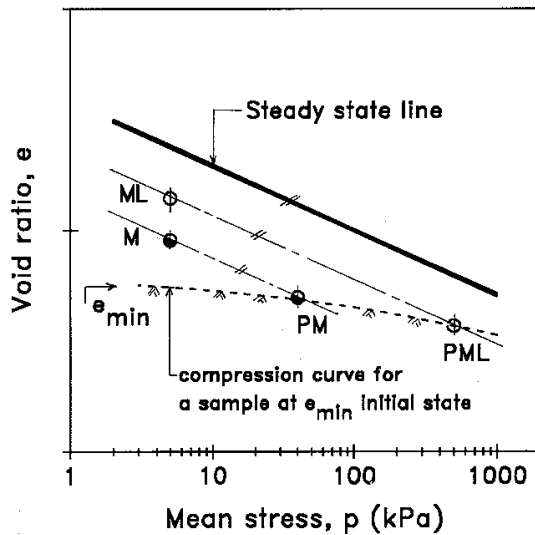


FIG. 9. Principle of reanalysis of data from 1g small-scale model tests to determine corresponding full-scale prototypes using the proposed approach. M, state of a small-scale model; PM, state of largest possible prototype that corresponds to a small-scale model of state M; ML, state of a small-scale model in a soil looser than state M; PML, state of largest possible prototype that corresponds to a small-scale model of state ML.

responding void ratio values,  $\gamma_p$  can be substantially larger than  $\gamma_m$ ),  $N$  can never be quite equal to  $n$  or vice versa.

Scott (1989) presented scaling relations similar to those presented in Table 3, but did not differentiate between the stress scale  $N$  and the geometric scale  $n$ , treating them as equal values, which, as mentioned, is not correct.

When the results of a physical small-scale model test are analyzed and applied to the behavior of a prototype structure, the Table 4 scaling relations will govern the calculated values of stress, strain, and displacement. Notice that the void ratio can also be scaled between the prototype and the physical model. Moreover, if the stress scale ratio  $N$  is equal to unity, and the model test is a conventional centrifuge test performed at the void ratio of the prototype, Table 4 reverts to Table 1.

#### Application to engineering practice

Physical modeling (performing small-scale tests) is a step in determining the behavior of a structure founded in a soil that is known to its in situ state. The initial state is determined by the slope and location of the steady state line and initial conditions of void ratio and mean stress. Engineering design of actual foundation structures involves theoretical modeling (analysis) of the behavior of the soil and structure. However, while the steady state line (slope and location) can be determined from laboratory testing of recovered samples, the in situ state of the soil is not that easily determined. Current engineering practice of site investigation, however, does not normally provide quantified information on the in situ void ratio (density) of cohesionless soils, let alone the in situ mean stress (combination of effective overburden stress and  $K_0$ ). In fact, no single existing in situ site-investigation tool can provide all the required information.

TABLE 4. Scaling relations of the physical modeling approach

|                  | Full-scale prototype | Model                        |
|------------------|----------------------|------------------------------|
| Linear dimension | 1                    | $n$                          |
| Area             | 1                    | $n^2$                        |
| Volume           | 1                    | $n^3$                        |
| Acceleration     | 1                    | 1                            |
| Stress           | 1                    | $N$                          |
| Strain           | 1                    | 1                            |
| Displacement     | 1                    | $n$                          |
| Force            | 1                    | $N n^2$                      |
| Void ratio       | $e_p$                | $e_m = e_p + \lambda \ln(N)$ |

NOTES:  $n$ , geometric scale ratio, linear dimension ratio,  $L_m/L_p$ ;  $N$ , stress scale ratio,  $p_m/p_p$  or  $\sigma'_m/\sigma'_p$ ;  $N/n = (1 + e_p)/(1 + e_m + \lambda \ln(N)) = [1 + e_m - \lambda \ln(N)]/(1 + e_m)$ ;  $e_m$ , void ratio of the model-scale soil;  $e_p$ , void ratio of the full-scale soil, the prototype condition;  $\lambda$ , slope ( $<0$ ) of the steady state line in the  $e - \ln(p)$  plane.

However, current research on the use of the piezocone and dilatometer is emphasizing these aspects. It is expected that the site investigation practice will soon be able to provide the designer with the necessary in situ data.

The scaling relations provided in Table 4 control the design of representative small-scale model tests. Three main areas of application of the proposed approach to physical modeling in engineering practice are identified and discussed below: (i) design of representative 1g small-scale model tests; (ii) reanalysis of data from 1g small-scale model tests; and (iii) improving the versatility of centrifuge facilities.

#### Design of representative 1g small-scale model tests

For a given full-scale prototype situation, a representative 1g small-scale model test can be designed so as to obtain test data (stress, strain, force, and movement), which represent the behavior of the prototype in accordance with the scaling rules listed in Table 4. The approach requires that the steady state line be determined in a series of consolidated undrained triaxial compression tests on the prototype soil. For details on how to establish the steady state line, see Poulos (1981), Castro et al. (1992), and Ishihara et al. (1991), for example. The physical size of the model, that is, the geometric scale  $n$ , is governed by several practical aspects, such as the size of the available testing facility and costs. Important technical aspects must also be considered, such as how to prepare a soil of the correct density to match the prototype. That is, the void ratio  $e_m$  of the soil in the small-scale model must be equal to or smaller than the upper-bound void ratio as governed by the maximum void ratio of the soil. The void ratio  $e_m$  of the soil to be used for the small-scale model is calculated by the condition that the upsilon parameter of the test soil is equal to that of the prototype soil. The void-ratio relation is given in Table 4. Some important technical aspects to consider are elimination of boundary effects, ensuring homogeneity of the soil, and many others common for the preparation and performance of model tests in general.

#### Reanalysis of data from 1g small-scale model tests

Data from 1g small-scale model tests conducted in a soil of the same density as that of the prototype are not useful for determining the behavior of the prototype structure. However,

the test results can be analyzed to determine the density of the prototype soil which would be representative for the particular model test. Of course, a reanalysis requires that the available soil data include information on the steady state of the soil.

For a prototype of specific dimensions in a soil of a given void ratio, the geometric scale must first be determined. Then, the stress scale is determined by means of the relations given in Table 4. Notice that there is an upper limit of the size of the prototype to fit a particular model test: the soil used in the model test must not be unrealistically dense; the density of the model test governs the density of the soil for the prototype, for which the soil must always be more dense than the soil for the model.

The minimum void ratio of the prototype soil is a practical upper limit for the initial void ratio in a model test. Then, an upper limit of the initial soil density is reached when the scales are such that the initial void ratio of the prototype soil needs to be at the maximum void ratio.

That the void ratio  $e_p$  of the soil in a prototype must not be smaller than the minimum void ratio has a very important practical significance. Figure 9 illustrates that the looser the soil used in the small-scale model, the larger the prototype (the larger the stress at the homologous points) to which the results of the small-scale model can be extrapolated. The test data obtained for the small-scale model indicated by state M in Fig. 9, for instance, can be extrapolated to different size prototypes, with the prototype state indicated by state PM as the upper limit, as controlled by the minimum void ratio and the compressibility of the soil. (The minimum void ratio is stress dependent and decreases somewhat with increasing mean stress. The curved line in Fig. 9 represents the compression curve of the soil.)

For a small-scale model tested in a soil looser than M, for example, as indicated by state ML, the test data can be extrapolated to larger prototypes, but there is always an upper limit represented by the intersection between the compression curve through the minimum void ratio line with the line parallel to the steady state line and offset by the  $\epsilon$  parameter (state PML correspondence to state ML).

The literature contains numerous results from 1g small-scale model tests on sand at its minimum void ratio. Such tests apply to no prototype (other than their being their own prototype), and the test data have little value.

*Improving the versatility of centrifuge facilities*

In the conventional centrifuge test, the stress scale ratio  $N$  must be unity. For large prototypes, the requirement to model details may render the model large enough to exceed the payload limit for the test. However, the authors' proposed approach to physical modeling does not require a stress scale ratio equal to unity. The approach allows the usefulness of small centrifuges to be extended beyond the conventional approach.

Figure 10 illustrates aspects of applying the new approach to centrifuge testing. Point P represents the initial state of the prototype soil. Assume that the initial mean stress for the prototype is, say, 100 kPa, and that the soil for the pertinent small-scale model M1 is to be prepared to match conditions for an initial mean stress of 2 kPa. (The void ratios of the prototype and the model soil are practically the same, and, of course, the void ratios must lie on the same compression curve of the soil.) Then, to perform a conventional centrifuge test, the centrifuge has to provide an accelera-

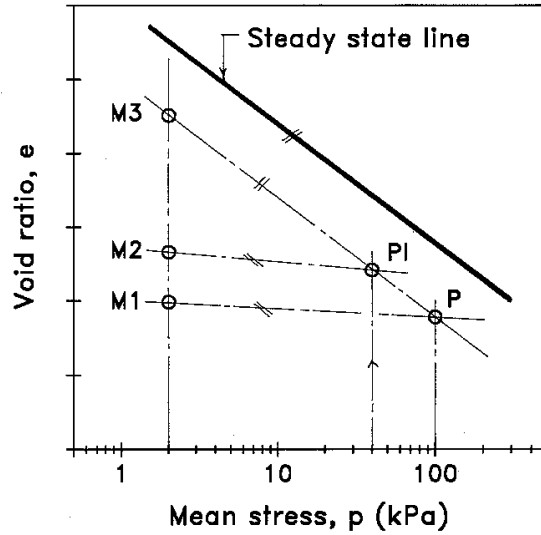


FIG. 10. Principles of improving versatility of centrifuge facilities using the proposed approach.

tion equal to the ratio between the values of initial mean stress, that is, 50g. However, the capacity of the particular hypothetical centrifuge (its upper acceleration limit for the particular size model) is, say, only 20g. So, by the scaling rules for the conventional approach given in Table 1, the test is not valid.

However, if the soil is prepared to a looser density, say, to the void ratio indicated for the model M2, instead, and this model is tested at 20g, then the test is representative for an "intermediate prototype" PI in agreement with the rules of Table 1. Because the  $\epsilon$  value for the soil of PI is the same as for P, the data for the "intermediate prototype" will then serve as a model test for the prototype at a stress scale of 2.5 by the rules of Table 4.

Moreover, in case of a centrifuge not capable of even the 20g spin, the initial void ratio of the soil for the model can be prepared for a higher value as determined by the particular conditions. In the extreme, the model test is performed under 1g conditions as illustrated by the state of the model test M3 in Fig. 10. Notice, as mentioned above, it may not be possible to prepare a soil at the loose density required.

Thus, the new approach allows the centrifuge to be used for testing models that are larger than indicated by the conventional scaling rules.

**Conclusions**

Because of the nonlinear stress-strain soil behavior and the dependency of behavior on initial level of confining stress, conventional tests of small-scale models in 1g condition may have little relevance to the behavior of the full-scale prototype. This difficulty is overcome by raising the stress level in the model to that of the prototype by testing in the centrifuge or by increased-gradient methods so that stresses in the model and prototype are equal at homologous points.

A new approach to small-scale testing of both 1g conditions and in the centrifuge is proposed. The steady state of deformation is selected as the reference. The principal requirement of the approach is that for a model and proto-

type to have comparative behavior at different initial level of stress, the initial soil states must be at equal proximity to the steady state line, that is, exhibit the same value of the  $v$  parameter, which is the void ratio difference to the steady state line. Then, when stresses are normalized to the initial mean stress, such models will in all aspects behave similarly to the prototype.

Scaling rules are presented (Table 4) that indicate the relations between stress, strain, and displacement for the model and the prototype in terms of geometric scale and stress scale.

The limits of scales of size and stress are governed by two requirements. First, for a certain loose condition of the prototype soil, there is an obvious limit of scales imposed because the density of the soil model can be no looser than the maximum void ratio. Second, the model soil must not be denser than that which corresponds to a prototype soil at the minimum void ratio.

Three main areas of application of the approach in engineering practice are identified: (i) design of representative 1g small-scale model tests; (ii) reanalysis of data from conventional small-scale tests; (iii) and improving the versatility of centrifuge facilities in recognition of the fact that the centrifuge test does not need to be performed at equal levels of stress, when designed according to the approach presented in this paper.

- Alarcon-Guzman, A., and Leonards, G.A. 1988. Discussion of "Liquefaction evaluation procedures," by S.J. Poulos, G. Castro, and J.W. France. *ASCE Journal of Geotechnical Engineering*, **114**(GT2): 232-236.
- Alarcon-Guzman, A., Leonards, G.A., and Chameau, J.L. 1988. Undrained monotonic and cyclic strength of sands. *ASCE Journal of Geotechnical Engineering*, **114**(GT10): 1089-1109.
- Altaee, A. 1991. Finite element implementation, validation, and deep foundation application of a bounding surface plasticity model. Ph.D. thesis, Department of Civil Engineering, University of Ottawa, Ottawa.
- Anderson, W.F., Hannah, R.H., Ponniah, D.A., and Shah, S.A. 1982. Laboratory scale tests on anchored retaining walls supporting backfill with surface loading. *Canadian Geotechnical Journal*, **19**: 213-224.
- Been, K., and Jefferies, M.G. 1985. A state parameter for sands. *Geotechnique*, **35**: 99-112.
- Been, K., Jefferies, M.G., and Hackey, J. 1991. The critical state of sands. *Geotechnique*, **41**: 365-381.
- Bishop, A.W., and Henkel, D.J. 1962. The measurements of soil properties in triaxial test. 2nd ed. Edward Arnold Ltd., London.
- Budhu, M., and Britto, A. 1987. Numerical analysis of soils in simple shear devices. *Soils and Foundations*, **27**: 31-41.
- Casagrande, A. 1936. Characteristics of cohesionless soils affecting the stability of slopes and earth fills. *Journal of the Boston Society of Civil Engineers*, **23**: 13-32.
- Castro, G., and Poulos, S.J. 1977. Factors affecting liquefaction and cyclic mobility. *ASCE Journal of the Geotechnical Engineering Division*, **103**(GT6): 501-516.
- Castro, G., Seed, R.B., Keller, T.O., and Seed, H.B. 1992. Steady-state strength analysis of lower San Fernando Dam slide. *ASCE Journal of Geotechnical Engineering*, **118**(GT3): 406-427.
- Chandler, R.J., and Martins, J.P. 1982. An experimental study of skin friction around piles in clay. *Geotechnique*, **32**: 119-132.
- Chari, T.R., and Meyerhof, G.G. 1983. Capacity of rigid single piles under inclined loads in sand. *Canadian Geotechnical Journal*, **20**: 849-854.
- Cheney, J.A. 1985. Physical modeling in geotechnical engineering. In *Proceedings of Centrifugal Workshop, 12th International Conference on Soil Mechanics and Foundation Engineering*, San Francisco, pp. 317-322.
- Cole, E.R. 1967. The behavior of soils in the simple shear apparatus. Ph.D. thesis, University of Cambridge, Cambridge, United Kingdom.
- Dennis, N. 1988. Discussion of "Liquefaction evaluation procedures," by S.J. Poulos, G. Castro, and J.W. France. *ASCE Journal of Geotechnical Engineering*, **114**(GT2): 241-243.
- Desai, C.S., and Siriwardane, H.J. 1984. Constitutive laws for engineering materials. Prentice-Hall Inc., Englewood Cliffs, N.J.
- Elsharnouby, B., and Novak, M. 1984. Dynamic experiments with group of piles. *ASCE Journal of Geotechnical Engineering*, **110**(GT6): 719-737.
- Fragaszy, R.J., and Lawton, E. 1984. Bearing capacity of reinforced sand subgrades. *ASCE Journal of Geotechnical Engineering*, **110**(GT10): 1500-1507.
- Graham, J., Raymond, G.P., and Suppiah, A. 1984. Bearing capacity of three closely-spaced footings on sand. *Geotechnique*, **34**: 173-182.
- Haliburton, D.A., and Lawmaster, J.D. 1981. Experiments in geotechnical fabric-reinforced soil behavior. *Geotechnical Testing Journal*, **4**: 153-160.
- Hegedus, E., and Khosla, V.K. 1984. Pullout resistance of H-piles. *ASCE Journal of Geotechnical Engineering*, **110**(GT9): 1274-1290.
- Ishihara, K., Verdugo, K., and Acacio, A.A. Characterization of cyclic behavior of sand and post-seismic stability analyses. In *Proceedings of the 9th Asian Regional Conference on Soil Mechanics and Foundation Engineering*, Bangkok. Vol. 2. pp. 45-67.
- Ko, H-Y. 1988. Summary of the state-of-the-art in centrifuge model testing. In *Centrifuge in soil mechanics*. Edited by W.H. Craig, R.G. James, and A.N. Schofield. A.A. Balkema, Rotterdam. pp. 11-18.
- Lade, P.V. 1982. Localization effects in triaxial tests on sand. In *Proceedings of a Conference on Deformation and Failure of Granular Materials*, Delft, The Netherlands. pp. 461-471.
- Lee, K.L., and Seed, H.B. 1967. Drained characteristics of sands. *ASCE Journal of the Soil Mechanics and Foundations Division*, **93**(SM6): 117-141.
- McRoberts, E.C., and Sladen, J.A. 1992. Observations on static and cyclic sand-liquefaction methodologies. *Canadian Geotechnical Journal*, **29**: 650-665.
- Milligan, G.W.E. 1983. Soil deformation near anchored sheet-pile walls. *Geotechnique*, **33**: 41-55.
- Pilecki, T.J. 1988. Discussion of "Liquefaction evaluation procedures," by S. Poulos, G. Castro, and J. France. *ASCE Journal of Geotechnical Engineering*, **114**(GT2): 246-247.
- Poulos, S.J. 1981. The steady state deformation. *ASCE Journal of the Geotechnical Engineering*, **107**(GT5): 553-562.
- Poulos, S.J., Castro, G., and France, J.W. 1988. Closure of discussion of "Liquefaction evaluation procedures." *ASCE Journal of Geotechnical Engineering*, **114**(GT2): 251-259.
- Pyke, R. 1988. Discussion of "Liquefaction evaluation procedures," by S.J. Poulos, G. Castro, and J.W. France. *ASCE Journal of Geotechnical Engineering*, **114**(GT2): 247-250.
- Richter, J.A., Demars, K.R., and Richards, R. 1984. Photoelastic analysis of laterally loaded rigid piles. *ASCE Journal of Geotechnical Engineering*, **110**(GT4): 548-551.
- Roscoe, K.H., and Poorooshasb, H. 1963. A fundamental principle of similarity in model test for earth pressure problems. In *Proceedings of the 2nd Asian Regional Conference on Soil Mechanics*, Bangkok, Thailand. Vol. 1. pp. 134-140.
- Roscoe, K.H., Schofield, A.N., and Wroth, C.P. 1958. On the yielding of soils. *Geotechnique*, **8**: 22-53.
- Schofield, A.N., and Wroth, C.P. 1968. *Critical state soil Mechanics*, McGraw-Hill, London.

- Scott, R.F. 1988. Physical and numerical models. *In Centrifuge in soil mechanics*, Edited by W.H. Craig, R.G. James, and A.N. Schofield. A.A. Balkema, Rotterdam. pp. 103–117.
- Scott, R.F. 1989. Essais en centrifuge et technique et de la modélisation. *Revue Française de Géotechnique*, Paris. No. 48, pp. 15–34.
- Selvadurai, A.P.S., and Rabbaa, S.A.A. 1983. Some experimental studies concerning the contact stresses beneath interfering rigid strip foundations resting on a granular stratum. *Canadian Geotechnical Journal*, **20**: 406–415.
- Sherif, M.A., Fang, Y.S., and Sherif, R.I. 1984.  $K_1$  and  $K_0$  behind rotating and non-yielding walls. *ASCE Journal of Geotechnical Engineering*, **110**(GT1): 41–56.
- Stroud, M.A. 1971. The behavior of sand at low stress levels in the simple shear apparatus. Ph.D. thesis, University of Cambridge, Cambridge, United Kingdom.
- Tan, T-S., and Scott, R.F. 1985. Centrifuge scaling consideration for fluid-particle system. *Geotechnique*, **35**: 461–470.
- Tatsuoka, F., and Ishihara, K. 1975. Drained deformation of sand under cyclic stress reversing direction. *Soils and Foundations*, **14**: 51–65.
- Tumay, M.T., Antonini, M., and Arman, A. 1979. Metal versus nonwoven fiber fabric earth reinforcement in dry sands: a comparative analysis of model tests. *ASTM. Geotechnical Testing Journal*, **2**: 44–56.
- Vaid, Y., Chung, E.K.F., and Keurbis, R.H. 1990. Stress path and steady state. *Canadian Geotechnical Journal*, **27**: 1–7.
- Whitman, R.V., and Arulanandan, K. 1985. Centrifuge model testing with dynamic and cyclic loads. *In Proceedings of Advances in the Art of Testing Soils under Cyclic Conditions*, Edited by V. Khosia. Detroit, Mich. pp. 255–285.
- Wroth, C.P., and Bassett, R.H. 1965. A stress-strain relationship for the shearing behavior of a sand. *Geotechnique*, **15**: 32–56.
- Yan, L., and Byrne, P.M. 1989. Application of hydraulic gradient similitude method to small-scale footing tests on sand. *Canadian Geotechnical Journal*, **26**: 246–259.
- Yan, L., and Byrne, P.M. 1991. Laboratory small-scale modeling tests using the hydraulic gradient similitude method. *In Proceedings of the Geotechnical Congress 1991*, Boulder, Colorado, June 1991. American Society of Civil Engineering, Special Technical Publication 27, Vol. II, pp. 827–838.
- Yazdanbod, A., O'Neill, M.W., and Aurora, R.P. 1984. Phenomenological study of model piles in sand. *ASTM. Geotechnical Testing Journal*, **7**: 135–144.
- Zelikson, A. 1969. Geotechnical model using the hydraulic gradient method. *Geotechnique*, **19**: 495–508.
- Zelikson, A. 1978. Rigid piles in sand under inclined forces; model tests using the hydraulic gradient similarity method. *Journal de mécanique appliquée*, **2**: 153–165.
- Zelikson, A. 1988. Hydraulic gradient simulation of sequences of pile driving and loading tests. *In Proceedings of the 3rd International Conference on the Application of Stress-Wave Theory to Piles*, Ottawa. Edited by B.H. Fellenius. Bitech Publishers, Vancouver. pp. 152–163.
- Zelikson, A., and Leguay, P. 1986. Some basic data on piles under static and dynamic loading from stress conserving models. *In Proceedings of the 3rd International Conference on Numerical Methods in Offshore Piling*, Nantes, France. pp. 105–124.